IEEE Access
Multidisciplinary | Rapid Review | Open Access Journal

Received September 11, 2019, accepted October 7, 2019, date of publication October 11, 2019, date of current version October 23, 2019.

Digital Object Identifier 10.1109/ACCESS.2019.2946644

A Heterogeneous Multi-Agent System Model With Navigational Feedback for Load Demand Management of a Zonal Medium Voltage DC Shipboard Power System

WENZENG DU[1,2], GENKE YANG[1,2], CHANGCHUN PAN[3], AND PEIFENG XI[4]

[1]Department of Automation, Shanghai Jiao Tong University, Shanghai 200240, China
[2]Collaborative Innovation Center for Advanced Ship and Deep-Sea Exploration, Shanghai 200240, China
[3]Department of Electronic Engineering, Shanghai Jiao Tong University, Shanghai 200240, China
[4]Shanghai Key Laboratory of Smart Grid Demand Response, Shanghai 200063, China

Corresponding author: Genke Yang (gkyang@sjtu.edu.cn)

This work was supported by the Natural Science Foundation of Shanghai under Grant 16ZR1416500, the Ministry of Industry and Information Technology of the People's Republic of China under Grant 2017YFA0700602, the Outstanding Talent Fund of Shanghai People's Insurance Bureau under Grant 2017116, and Shanghai Science and Technology Commission Project under Grant 18DZ1203502.

ABSTRACT Increased demand of electric ship power with emerging requirements for serving highly dynamic loads at limited power sources, has motivated the development of medium voltage DC shipboard power systems. As different types of power converters can be involved in the same system, advanced load management scheme is required to ensure stable and optimal operation under various conditions. In this paper, a heterogeneous multi-agent system model is established for the load demand management of a zonal medium voltage DC shipboard power system, where different types of DC-DC converters with diverse conversion ratios are considered as heterogeneous agents. Then, a flocking based cooperative control protocol is designed to achieve the group objective, where navigational feedback is introduced to ensure that each agent runs within a limited range. Finally, numerical simulations are conducted to verify the performance of the proposed model. Compared with the existing work, our contribution lies in: 1) The heterogeneous multi-agent system model we formulated for a combination of DC-DC converters with different types and diverse voltage levels is more consistent with the actual power system and each converter can be controlled individually according to load ratings and priorities; 2) The modified navigational feedback with the function of confining the lower and upper bound of agents can significantly improve the control effect of the cooperative control protocol.

INDEX TERMS Medium voltage DC shipboard power system, heterogeneous multi-agent system model, load demand management, DC-DC converter, navigational feedback.

I. INTRODUCTION

An ongoing trend of ship power system (SPS) development is the integration of propulsion with the electrical system, since the requirement of propulsion power and other high energy equipment is not always synchronous [1]. One of the benefits of the integrated power system is to give a maximum capacity in consideration of the space and weight constraints. However, with the increasing demand for high power mission systems, it becomes inevitable that the generators may easily be overloaded, which consequently leads to system instability [2]. Although energy storage elements are widely used in power systems for smoothing the power fluctuations, the size, weight and potential hazards limit their extensive use on ships. In order to make SPS operate properly in various conditions for a wide range of power demand, it is essential to balance the load demand and power generation in real time. Therefore, an efficient load management method is needed for SPS to deal with the complicated and fluctuating power requirements.

The associate editor coordinating the review of this manuscript and approving it for publication was Sanjeevikumar Padmanaban.

Although traditional AC architectures have enabled economical and reliable power systems due to the convenience of electric transformers, recent successes in the development of fast switching medium-voltage power semiconductors promote electrical equipment with high efficiency and high power density through the use of DC architectures [3]. The load that SPS must provide has experienced considerable growth with the introduction of high-power combat systems and the electrification of auxiliary equipment, which naturally results in the adoption of medium voltage DC (MVDC) architecture for future SPS [4]. In early 21st century, the US navy first proposed the concept of zonal ship design [5]. Combing the advantages of zonal structure and MVDC interface, the work in [6] and [7] illustrates a conceptual zonal MVDC distribution power system in which every power source and every electrical load are connected to MVDC bus via power converters. It is expected that the function of future electric SPS should consist of control, stability and protection, by utilizing the inherent control ability of the power converters all over the system. However, the control concept for a system of high density power electronics is still limited, and new concept of control is urgently needed.

Conventional load management in terrestrial power systems mainly focus on reducing the operating cost and maintaining the reliability of the electric network by adjusting or controlling the load demand while achieving certain objectives, such as maximizing the profit margin [8], reducing the operating cost or the peak load [9], [10]. Distinct from the terrestrial power system, SPS has finite power sources while including a large number of dynamic loads and time-sensitive components [11], which requires the determination time of the controller to be small. Most centralized control schemes need some sort of global information of the structure of the power network [12]. Furthermore, centralized control scheme lacks adaptivity to structural changes and may encounter a single point of failure [13]. As one of the most popular decentralized approaches, multi-agent system(MAS) technology has been applied to address challenges in power engineering, including monitoring and diagnosis, distributed control and power system protection [14], etc. For electric SPS, MAS has also been applied to load restoration [13], system reconfiguration [15], fault detection [16], etc.

There have been some significant work on load management using multi-agent technology [11], [17]. Initially, Feng *et al.* [11] formulated the dynamics of the power conversion module (PCM) into a reduced-order agent model, agents were considered homogeneous since all the converters in PCM were considered identical. The advantage of this strategy is the convenience of modelling and design of control protocol, while the disadvantage is the low accuracy since the agent is simple and all the converters are aggregated together. In their latest work, Feng *et al.* [17] modelled all the primary electrical components in SPS as heterogeneous agents with converters and loads modelled separately. Despite the complicated topology, it does improve the accuracy of agent models.

The novelty of this work lies in: 1) Different types of DC-DC converters with diverse conversion ratios are modelled as heterogeneous agents, which gives consideration to both accuracy and versatility; 2) A modified navigational feedback, with the function of confining the lower and upper bound of the agents, is designed for achieving a superior control effect of the multi-agent cooperative control protocol.

The rest of this paper is organized as follows. In Section II, a notional zonal MVDC SPS is introduced as the object of our study. Section III shows the agent model formulation and the group objective of the multi-agent system in zonal area. In Section IV, a flocking based cooperative control protocol with modified navigational feedback is designed for optimal control of the multi-agent system model. Numerical simulations are presented in Section V to validate the performance of the proposed method. Then, a brief discussion about the improvements of our method is presented in Section VI. Finally, conclusions and future work are stated in Section VII.

II. ZONAL MVDC SHIPBOARD POWER SYSTEM MODEL

The conventional structure of the distribution system on shipboard is radial, and its capacity is usually small. However, with the development of high-energy equipment and the increasing power demand for flexible maneuverability, it becomes imperative to give a maximum capacity in consideration of space and weight constraints [18]. In the last few years, researchers have proposed some innovative distribution structures such as ring structure [12] and zonal structure [5], [6], [19]. Yet there have been numerous work on the study of the ring structure distribution system. Our study is focused on zonal distribution SPS, which is regarded as a future shipboard power distribution architecture.

Referring to the IEEE standard recommended for MVDC power system on ships [6], we propose a scaled-down model of a zonal MVDC SPS as shown in Fig.1. The model in Fig.1 is presented in a one-line diagram as a high-level view to favor readability. The architecture of such a zonal MVDC SPS is able to maximize operational capability even under extremely adverse conditions.

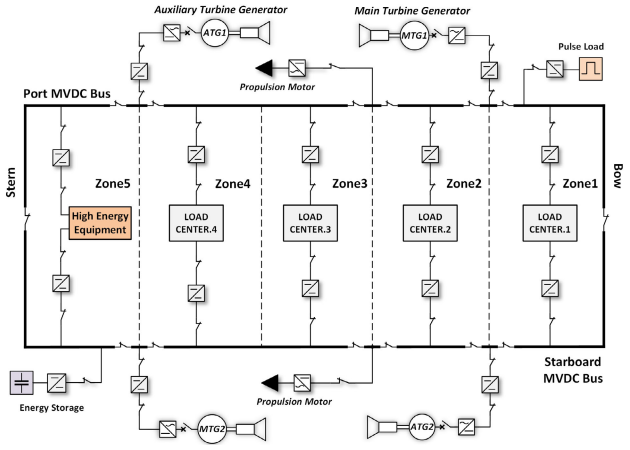

FIGURE 1. Scaled-down model of a zonal MVDC SPS.

For the power sources, there are two main turbine generators, each of which produces 36MW power at 4.16 kV, 240 Hz [20], and two auxiliary turbine generators producing 4MW power each. One main and one auxiliary turbine generator are connected to each longitudinal bus. Downstream of each generator is a three-phase circuit breaker. Behind each three-phase breaker is the AC-DC converter that powers the main DC bus at 5.5 kV DC.

Typically, power system survivability can be enhanced by opening the bow and stern disconnect switches to create a 'split-plant' configuration [6].

The main MVDC bus serves two propulsion motors (36.5MW for each) and five zones. Ship service loads are distributed in four zones from bow to stern along the ship and fed by 1kV DC power from either port bus or starboard bus, after the conversion of the bus-tie converters [21]. Zone 5 represents the deck house and the location for high-energy equipment [6]. The diagram of the load center is shown in Fig.2. The main part of the load center is an integrated PCM1 which gets the power supply from either starboard bus or port bus. Each PCM1 consists of three DC-DC converters which convert 1000V DC voltage into different levels of load voltages [11], such as 375V, 650V, 800V or 1500V DC.

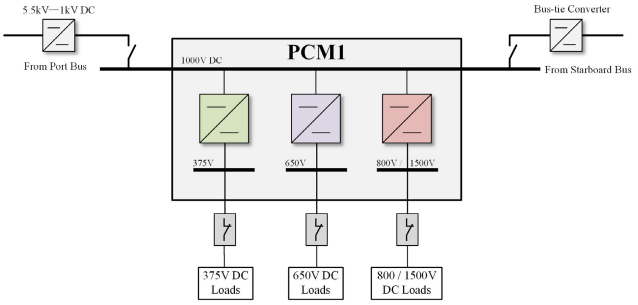

FIGURE 2. Diagram of the load center (PCM1).

In the zonal MVDC SPS, every power source and every load are connected to DC bus through power converters. The future electric SPS aims to have control, stability and protection integrated into one process. It is promising to match the load demand with power generation by controlling the power converters. In this context, the research is to model the dynamics of power conversion module for the purpose of balancing the load demand with the available power supply in zones by controlling the switch status of service loads.

III. MULTI-AGENT SYSTEM MODEL FOR LOAD MANAGEMENT IN ZONAL AREA

Although centralized control methods already have mature applications in shipboard power systems, decentralized methods still have its research significance as a backup and supplement for the overall power management system, especially in zonal MVDC SPS. As a representative decentralized control method, MAS technology has several advantages in the following scopes:

- Reliability. The system can maintain operating capability as much as possible in the event of the loss of communication or control links.
- Scalability. MAS is more adaptive to the modular-designed zonal MVDC SPS. It can easily integrate new components without changing the existing framework.
- Complexity. The design complexity only increases proportionally when the number of agents increases, while centralized method increases exponentially.

Moreover, an all-electric shipboard power system is a high-order multivariable process whose dynamics is influenced by a wide range of devices with different characteristics and response rates [22]. It is necessary to find an appropriate object whose dynamic can represent the supply and demand relationship of SPS and is easy to be modelled. For the zonal MVDC SPS shown in Fig.1, there are four load centers in the zonal area, and each load center has a similar architecture (as shown in Fig.2), where the DC-DC converters act as an intermediate link between the power sources and the service loads, the control of converters is the key of demand side load management in zonal area. So the modelling of the DC-DC converter is inevitable.

A. SCHEMATIC OF THE DC-DC CONVERTER

DC-DC converter is a type of electronic power converter which is able to convert a source of direct current from one voltage level to another [23]. Considering the characteristics of the power distribution system in MVDC SPS, representative DC-DC converters such as buck converter and boost converter are considered in this work.

A buck converter is a DC-DC power converter which steps down voltage from its input to its output. Typical buck converter consists of two switched-mode semiconductors, a transistor and a diode, and at least one energy storage element, as shown in Fig.3(a).

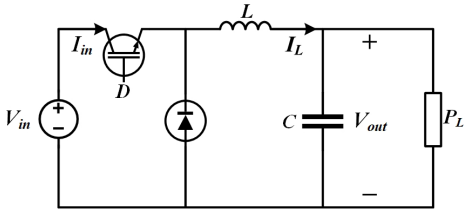

(a) Buck converter with constant power load

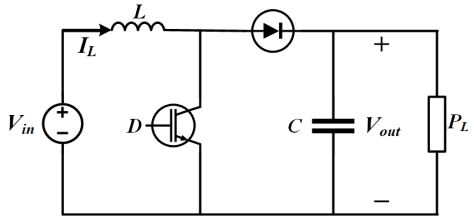

(b) Boost converter with constant power load

FIGURE 3. Schematic circuit diagram of the DC-DC converter.

The efficiency of the buck converter can be remarkably high, here the efficiency of the buck converter is assumed to be 100%, which means there is no power loss in the DC-DC power conversion process. The load downstream is modelled as a constant power load since its voltage is tightly controlled by the converter [24].

In consideration of the current continues mode of the inductor and the periodicity of the transistor, the input-output relationship of the buck converter can be be expressed in a time-average model [25]:

$$\begin{cases} L\dfrac{dI_L}{dt} = DV_{in} - V_{out} \\ C\dfrac{dV_{out}}{dt} = I_L - \dfrac{P_L}{V_{out}} \end{cases} \tag{1}$$

where I_L is the current of the inductor L. V_{in} is the input voltage of the buck converter, which is kept constant at 1000V DC. $V_{out} = 375\text{V}, 650\text{V}$ and 800V are the output voltages of the converter, which directly serve the downstream DC loads. D is the duty cycle of the transistor, which ranges from 0 to 1. In this paper, D is considered to be constant for a given output voltage. L and C are inductance and capacitance of the buck converter. P_L is the power of the entire constant power loads, which can be expressed as:

$$P_L = \sum_i (\sigma_i \cdot P_{L_i}) \tag{2}$$

where P_{L_i} is the rated power of the i_{th} service load. σ_i is the switch status of the corresponding load, $\sigma_i \in \{0, 1\}$, where 0 represents the switch is off and the corresponding load is not at service, while 1 represents the opposite.

There is a linear relationship between the input current and the inductance current of the buck converter under the time-average model, which is:

$$I_{in}(t) = DI_L(t) \tag{3}$$

A boost converter is devised to step up voltage (while stepping down current) from its input to output, where the schematic circuit diagram is shown in Fig.3(b). The dynamic model of the boost converter can be represented as:

$$\begin{cases} L\dfrac{dI_L}{dt} = V_{in} - (1-D)V_{out} \\ C\dfrac{dV_{out}}{dt} = (1-D)I_L - \dfrac{P_L}{V_{out}} \end{cases} \tag{4}$$

The physical meanings of the parameters are all the same with the buck converter's, while the output voltage $V_{out} = 1500V$.

B. AGENT MODEL FORMULATION

The proposed zonal MVDC SPS is evidently a typical cyber-physical system which closely integrates monitoring, communication, computation and real time control.

Agent model formulation of SPS in zonal area involves physical layer and communication layer. For the physical layer, the DC power network in zonal area is partitioned into four zones, each zone has a similar topology as shown in Fig.4(a), which is a port DC distribution bus, a starboard DC distribution bus, a PCM1 that consists of three DC-DC converters and several service loads.

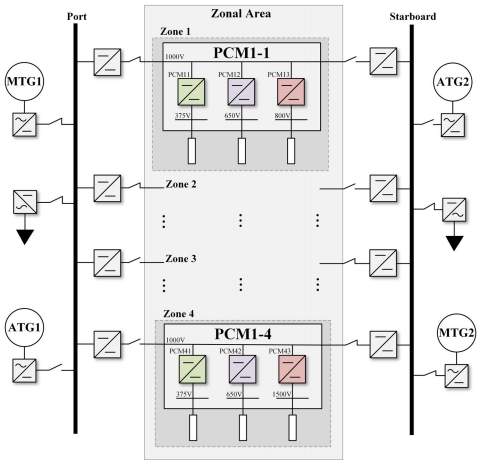

(a) System physical layer

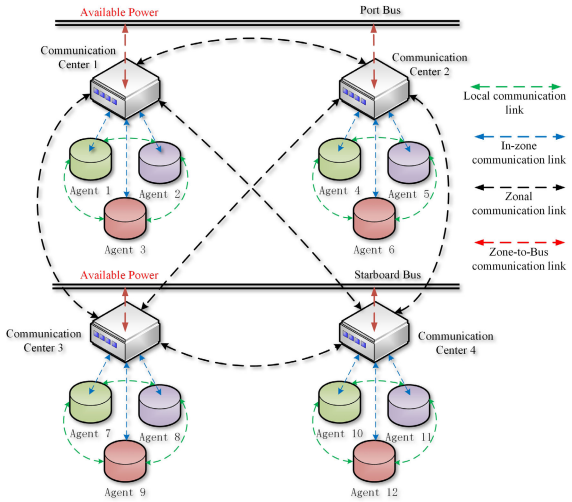

(b) System communication layer

FIGURE 4. Multi-agent system model for load management in zonal area.

The relationship between power supply and load demand in each zone can be reflected by the dynamics of the DC-DC converters. Therefore, each DC-DC converter is modelled as an agent, and a PCM1 is formulated as a set of three agents.

Established on the basis of the power network, the communication network of each agent is shown in Fig.4(b), agent 1 to agent 12 represents PCM11 to PCM43 respectively. Since PCM1 has the function of controlling and monitoring the circuit parameters of the service loads, each PCM1 is regarded as a communication center. Each agent locally measures its operating state and communicates with its neighbors, and the information flow is depicted by the green dash line. In-zone communication between the agent and the communication center is bidirectional, as depicted by the blue dash line.

Cross-zone communication is conducted through communication centers, and it can be viewed as a fully-connected network, which is depicted by the black dash lines. Finally, the communication between the in-zone load demand and the external available power is conducted through the MVDC bus and the communication centers, as depicted by the red dash lines.

In this paper, each buck converter together with its belonging loads is modelled as an agent, and to coordinate with the multi-agent algorithm, the inductor current I_L and its current changing rate are adopted as the state variables:

$$\begin{cases} x(t) = I_L(t) \\ y(t) = (DV_{in} - V_{out}(t))/L \end{cases} \tag{5}$$

Thus the time-average model (1) can be transformed into a second order dynamic system with multi-agent motion, which is:

$$\begin{cases} \dot{x}(t) = y(t) \\ \dot{y}(t) = -\dfrac{1}{LC}[x(t) - \dfrac{1}{DV_{in} - Ly(t)}\hat{u}(t)] \end{cases} \tag{6}$$

where $x(t)$ is the induction current of the buck converter, and $y(t)$ is the changing rate of $x(t)$. $\hat{u}(t) = \sum(\sigma_i P_{L_i})$ is related to the demand of the constant power load, where σ_i is the switch status of each load.

With the same principle applies to the boost converter,

$$\begin{cases} x(t) = I_L(t) \\ y(t) = (V_{in} - (1-D)V_{out}(t))/L \end{cases} \tag{7}$$

The dynamic model (4) can be transformed into

$$\begin{cases} \dot{x}(t) = y(t) \\ \dot{y}(t) = -\dfrac{1}{LC}[(1-D)^2 x(t) - \dfrac{1}{V_{in} - Ly(t)}\hat{u}(t)] \end{cases} \tag{8}$$

For the buck converter agents, let $u(t) = -\frac{1}{LC}[x(t) - \frac{1}{DV_{in}-Ly(t)}\hat{u}(t)]$. For the boost converter agents, let $u(t) = -\frac{1}{LC}[(1-D)^2\, x(t) - \frac{1}{V_{in}-Ly(t)}\hat{u}(t)]$. Give an overall consideration of the dynamic models (6) and (8), the collective dynamics of the multi-agent model can be expressed as:

$$\begin{cases} \dot{\boldsymbol{x}}(t) = \boldsymbol{y}(t) \\ \dot{\boldsymbol{y}}(t) = \boldsymbol{u}(t) \end{cases} \tag{9}$$

where $\boldsymbol{x}(t), \boldsymbol{y}(t), \boldsymbol{u}(t) \in \mathbb{R}^{M \cdot N}$,

$$\begin{aligned} \boldsymbol{x}(t) &= [x_{11}(t), \cdots, x_{1N}(t), \cdots, x_{M1}(t), \cdots, x_{MN}(t)]^T, \\ \boldsymbol{y}(t) &= [y_{11}(t), \cdots, y_{1N}(t), \cdots, y_{M1}(t), \cdots, y_{MN}(t)]^T, \\ \boldsymbol{u}(t) &= [u_{11}(t), \cdots, u_{1N}(t), \cdots, u_{M1}(t), \cdots, u_{MN}(t)]^T. \end{aligned}$$

$x_{ij}(t)$ and $y_{ij}(t)$ are state variables that represent the induction current and current changing rate of the corresponding DC-DC converter agent respectively. $u_{ij}(t)$ is the control variable used to characterize the control motion of the multi-agent system. M is the number of the load zones, while N is the number of the converters in each PCM1. In this paper, there are 12 converter agents contained in 4 PCM1, that is to say, $M = 4$ and $N = 3$.

Referring to (3), the current of each PCM1 can be expressed as the sum of its belonging converter agents:

$$I_i(t) = \sum_{j \in K^i} D_j x_{ij}(t) + \sum_{j \in T^i} x_{ij}(t) \tag{10}$$

where $I_i(t)$ represents the input current of each PCM1, $x_{ij}(t)$ represents the inductor current of each converter agent, D_j is the duty cycle of the corresponding buck converter. The set of the buck converter agents is denoted by K, which is a two-dimensional array. K^i represents the i_{th} row of array K, and the set of the boost converter agents is denoted by T.

C. GROUP OBJECTIVE OF THE MULTI-AGENT SYSTEM

Load demand management is the process of balancing the power supply with the electrical load by controlling the load rather than adjusting the power generation.

As for the zonal MVDC SPS, we aim to maximize load power for the zonal load centers while ensuring certain operating constraints such as rated output power of the generators and stable operation of the propulsion motors, etc.

The active power consumed by PCM1-1, PCM1-2, PCM1-3 and PCM1-4 are defined as $P_1(t)$, $P_2(t)$, $P_3(t)$ and $P_4(t)$ respectively. The total available power for zonal load centers is defined as $P_{total}(t)$, which means $\sum_{i=1}^{M} P_i(t)$ is no more than $P_{total}(t)$. The power available for port bus and starboard bus are expressed as $P_{pBus}(t)$ and $P_{sBus}(t)$ respectively. Due to the 'split-plant' configuration [6] of the zonal SPS, PCM1-1 and PCM1-2 are specified to be connected with the port side DC bus, while PCM1-3 and PCM1-4 are connected with the starboard side DC bus.

As mentioned above, the group objective of the multi-agent system is to maximize the load demand in affordable time subject to the available power supply and system operating constraints. Accordingly, the objective function and the constraints of the multi-agent model can be expressed as (11):

$$\begin{aligned} &\max \sum P_i(t) \\ &s.t. \sum P_i(t) \le P_{total}(t) \\ &\quad \sum_{i \in pBus} P_i(t) \le P_{pBus}(t) \\ &\quad \sum_{i \in sBus} P_i(t) \le P_{sBus}(t) \\ &\quad P_i(t) = V_{in} \cdot I_i(t) \\ &\quad \dot{x}_{ij}(t) = y_{ij}(t) \\ &\quad \dot{y}_{ij}(t) = u_{ij}(t) \end{aligned} \tag{11}$$

In section II, it is assumed that the input voltage V_{in} of each PCM1 is well-controlled and kept constant at 1kV DC. The relation of current $I_i(t)$ and $x_{ij}(t)$ is expressed in (10). So the objective function of the multi-agent system model can

finally be formulated as (12):

$$\begin{aligned}
&\max \sum I_i(t) \\
&s.t. \sum I_i(t) \le I_{total}(t) \\
&\sum_{i\in pBus} I_i(t) \le I_{pBus}(t) \\
&\sum_{i\in sBus} I_i(t) \le I_{sBus}(t) \\
&I_i(t) = \sum_{j\in K^i} D_j x_{ij}(t) + \sum_{j\in T^i} x_{ij}(t) \\
&\dot{x}_{ij}(t) = y_{ij}(t) \\
&\dot{y}_{ij}(t) = u_{ij}(t)
\end{aligned} \tag{12}$$

where $I_{total}(t)$ is the total available current of the multi-agent model. $I_{pBus}(t)$ and $I_{sBus}(t)$ are the available current of port bus and starboard bus respectively.

IV. FLOCKING BASED COOPERATIVE CONTROL PROTOCOL

In this paper, different types of DC-DC converters with diverse voltage levels are formulated as heterogeneous agents. The group objective of the agents is to maximize the energized loads, which is equivalent to maximize $\sum I_i(t)$. The available power capacity constraint is to ensure that the total current input of the load centers is no more than $I_{total}(t)$. The operating constraints of the port side and starboard side bus are considered as $\sum_{i\in pBus} I_i(t) \le I_{pBus}(t)$ and $\sum_{i\in sBus} I_i(t) \le I_{sBus}(t)$.

It is evident that the formation of the dynamical system in (9) is compatible with flocking algorithm. To solve the problem (12) in a multi-agent manner, a new control protocol is needed. Flocking is a biological phenomenon which a large number of interacting agents with a common group objective perform a collective behaviour [26]. In flocking algorithm, each agent is linked with a control input that consists of three terms [26]:

$$u_{ij}(t) = f_{ij}^g + f_{ij}^d + f_{ij}^\gamma \tag{13}$$

$f_{ij}^g = -\nabla_{x_{ij}} E_p(x)$ is a gradient-based term, where $E_p(x)$ is the collective potential function of all the agents, f_{ij}^d is a consensus term that acts as a damping force, and f_{ij}^γ is a navigational feedback due to the group objective. To achieve the objective of the multi-agent system, the control variable $u_{ij}(t)$ should be well designed.

A. COLLECTIVE POTENTIAL FUNCTION

The collective potential function of a group of agents is a nonnegative function with the property that any solution of the set is closely related to a local minimum and vice versa [26].

To satisfy the system operating constraints, the collective potential function $E_p(x)$ is designed as follows:

$$E_p(\boldsymbol{x}) = J_1(\boldsymbol{x}) + J_2(\boldsymbol{x}) + J_3(\boldsymbol{x}) \tag{14}$$

where $J_1(x)$ is the potential energy function to maximize the service load demand while satisfying the total available power capacity constraints. $J_2(x)$ and $J_3(x)$ are penalty functions to ensure the port side and starboard side bus operating constraints. The potential energy function $J_1(x)$ is designed as:

$$J_1(\boldsymbol{x}) = c \cdot (\sum_i I_i(t) - I_{total}(t))^2 \tag{15}$$

where $I_i(t)$ is the current of each PCM1 and is expressed in (10), and $\sum_i I_i(t)$ is the current demand of all the agents. c is a positive constant to regulate the optimization speed. Since the objective of the system is to maximize $\sum_i I_i(t)$ and $\sum_i I_i(t) \le I_{total}(t)$, the function will reach its global minimum along gradient descent when $\sum_i(\sum_{j\in K^i} D_j x_{ij} + \sum_{j\in T^i} x_{ij}) = I_{total}(t)$.

The penalty function $J_2(x)$ and $J_3(x)$ are designed as:

$$\begin{aligned}
J_2(\boldsymbol{x}) &= q_1(\sum_{i\in pBus} I_i(t) - I_{pBus}(t) + |\sum_{i\in pBus} I_i(t) - I_{pBus}(t)|)^2 \\
J_3(\boldsymbol{x}) &= q_2(\sum_{i\in sBus} I_i(t) - I_{sBus}(t) + |\sum_{i\in sBus} I_i(t) - I_{sBus}(t)|)^2
\end{aligned} \tag{16}$$

q_1 and q_2 are positive constants used to adjust the penalty function. For $J_2(x)$, it increases quadratically when $\sum_{i\in pBus} I_i(t) > I_{pBus}(t)$, otherwise it remains to zero. And $J_3(x)$ is the same.

B. GRAPH LAPLACIAN

A consensus protocol is an interaction rule that specifies the information exchanges between an agent and its neighbors on the network [27]. Graph laplacian is a consensus term appears in analysis of velocity matching of agents in flocks [26].

For the zonal MVDC SPS, the equivalent multi-agent model in Fig.4 can be viewed as a two-layer graph, where the upper layer is the PCM1s and the lower layer is the heterogeneous agents. For the lower layer, each agent can obtain the information of other agents provided that the agents are included in the same PCM1. For the upper layer, each PCM1 acts as a communication center, which is able to get the information of the total power capacity via the connected MVDC bus. With consideration of the previous assumption, PCM1-1 and PCM1-2 have access to the information flow in the port bus, while PCM1-3 and PCM1-4 have access to the information flow in the starboard bus. Consider a graph G of order n has the same topology as the multi-agent system, the adjacency matrix of G is $A = [a_{ij}]$, the degree matrix of G is a diagonal matrix $\Delta = \Delta(A)$. The graph laplacian matrix L_G is defined as [26]

$$L_G = \Delta(A) - A \tag{17}$$

Thus the elements of L_G is given by:

$$L_{ij} = \begin{cases} deg(v_i) & i = j \\ -1 & i \ne j, j \in N_i \\ 0 & otherwise \end{cases} \tag{18}$$

where $deg(v_i)$ is the degree of vertex i, N_i is the set of neighbours of i [26].

In the multi-agent system, state variable y of each agent is required to reach a consensus with its neighbours. As the inputs of the DC-DC converters in the same PCM1 are paralleled, the current ramp rates need to reach an equilibrium.

C. NAVIGATIONAL FEEDBACK

In the multi-agent system, feedback is needed to make sure that the agents approach the same group objective and avoid fragmentation [26]. The information of the state variables x and y are needed to develop the feedback correction. In this paper, the navigational feedback is designed as:

$$f_{ij}^{\gamma}(x_{ij}, y_{ij}) = -k_1(x_{ij} - max(x_{ij}, x_{ij}^{min})) - k_2(x_{ij} - min(x_{ij}, x_{ij}^{max})) - k_3(y_{ij} - \dot{P}_{total}(t)) \tag{19}$$

where $max[\cdot]$ returns a maximum value and $min[\cdot]$ returns a minimum value, x_{ij}^{min} is the minimum current requirement of the corresponding agent and x_{ij}^{max} is the maximum current requirement of the corresponding agent. k_1, k_2 and k_3 are positive constants used to regulate the feedback rates of the agents.

The three terms in (19) are used to ensure that x_{ij} is not less than its required lower bound, x_{ij} does not exceed its required upper bound, and the changing rate of the agent is consistent with system's changing rate $\dot{P}_{total}(t)$ respectively. In the case of a constant input voltage, state variable y of each agent is physically equivalent to the demand power ramp rate, which is necessary to be kept consistent with the generation power ramp rate $\dot{P}_{total}(t)$ for avoiding instability and the excessive employment of energy storage elements.

D. COOPERATIVE CONTROL PROTOCOL

Finally, the dynamics of the multi-agent model applying the control protocol (13) is formulated in the following form:

$$\begin{cases} \dot{x}_{ij}(t) = y_{ij}(t) \\ \dot{y}_{ij}(t) = u_{ij}(t) \end{cases} \tag{20}$$

$$u_{ij}(t) = -\frac{\partial E_p(\boldsymbol{x}(t))}{\partial x_{ij}(t)} - L_G{}^r \cdot \boldsymbol{y}(t) - f_{ij}^{\gamma}(x_{ij}, y_{ij}) \tag{21}$$

where $E_p(\boldsymbol{x}(t))$ is the artificial potential function described in (14)-(16). $L_G{}^r$ is the r_{th} row of the Laplacian matrix L_G defined in (17)(18), and $r = 3(i-1)+j$. $f_{ij}^{\gamma}(x_{ij}, y_{ij})$ is the navigational feedback defined in (19).

Since $u_{ij}(t)$ is the control signal of the multi-agent system, it should be transformed into the original control signal $\hat{u}_{ij}(t)$ to control the switch status of service loads. Referring to (6) and (8), the original control signal $\hat{u}_{ij}(t)$ of the loads in zonal area can be calculated by:

$$\hat{u}_{ij}(t) = \begin{cases} (LCu_{ij}(t) + x_{ij}(t))(D_j V_{in} - Ly_{ij}(t)) & j \in K^i \\ (LCu_{ij}(t) + (1-D_j)^2 x_{ij}(t))(V_{in} - Ly_{ij}(t)) & j \in T^i \end{cases} \tag{22}$$

Once $u_{ij}(t)$ is confirmed, the configuration of the switch status can be modelled as a single knapsack problem, and it is a NP-hard problem. While in the actual operating conditions, the service loads are always ranked by their priorities, so that the configuration of the load switch can be viewed as a sequential operation.

V. NUMERICAL SIMULATIONS

This section discusses the numerical simulation of the proposed flocking based cooperative control protocol for load demand management of the zonal MVDC SPS.

The state parameters in DC zones such as voltage class, load ratings and load priorities are considered as shown in Table 1 [11]. The consumed power of propulsion load and high-energy equipment changes with ship operation conditions, where the propulsive power is positively correlated to ship speed, and most of the high-energy equipment is assumed to be pulse loads. Without loss of generality, it is assumed that during normal conditions, two ATGs are not in service, so that the total power generation is 72MW. In the case of 'split-plant' configuration, it is assumed that the port side and starboard side power available for the load zones are 2MW.

TABLE 1. The state parameters of loads in DC zones.

PCM Number	Voltage Class(DC)	Load Quantity	Load Rating(MW)	Load Priority
PCM11	375V	1	0.1	Vital
		4	0.05	Semi-Vital
PCM12	650V	1	0.2	Vital
		6	0.05	Semi-Vital
PCM13	800V	1	0.1	Vital
		5	0.02	Semi-Vital
PCM21	375V	1	0.1	Vital
		3	0.06	Semi-Vital
PCM22	650V	1	0.2	Vital
		6	0.05	Semi-Vital
		1	0.05	Non-Vital
PCM23	1500V	1	0.1	Vital
		4	0.06	Semi-Vital
PCM31	375V	1	0.1	Vital
		3	0.05	Semi-Vital
PCM32	650V	1	0.2	Vital
		4	0.05	Semi-Vital
		5	0.04	Non-Vital
PCM33	800V	1	0.1	Vital
		2	0.1	Semi-Vital
PCM41	375V	1	0.1	Vital
		5	0.04	Semi-Vital
PCM42	650V	1	0.2	Vital
		5	0.04	Semi-Vital
PCM43	1500V	1	0.1	Vital
		5	0.05	Semi-Vital

The default parameters of the cooperative control protocol are chosen as follows:

$$c = 10, \quad q_1 = q_2 = 10, \; k_1 = k_2 = 100, \; k_3 = 10$$
$$L = 0.094H, \quad C = 0.0593F$$

Next, a case study including several typical operating conditions is presented to test the effect of the control protocol. In this case, the power consumed by the propulsion load decreased linearly from 70.4MW to 68MW from 2s to 6s, and thereafter maintained at 68MW. In order to provide energy for the pulse loads, system was required to charge energy storage elements with 2.4MW from 12s to 17s, and then decreased to 1MW.

Since the total power generation is 72MW, the power available for the zonal load centers increased from 1.6MW to 4MW from 2s to 6s, after 6 seconds of stable operation, it decreased to 1.6MW instantaneously, and returned to 3MW at 17s.

A. COMPARISON WITH THE HOMOGENEOUS METHOD

The homogeneous multi-agent method proposed in [11] is presented here as a comparison. With the homogeneous multi-agent modelling method, each zonal PCM1, which contains three DC-DC converters and several electrical loads, is modelled as an integrated agent. The dynamics of each agent is identical, which explains its homogeneity. Similarly, their objective is to maximize load demand subjecting to system operating conditions. While the communication topology of the homogeneous agents can be viewed as a fully-connected graph with four vertices and six edges, where each agent is able to communicate with each other.

For the fairness of comparison, the artificial potential function and the parameters of the control protocol are chosen as the same. At the initial state, the total available power in zones is 1.6MW, each load center is prioritized to ensure the power supply of vital loads. The simulation result is shown in Fig.5. We can see that both of the methods are able to maintain the balance between power supply and load demand precisely when the available power changes gently from 0s to 12s.

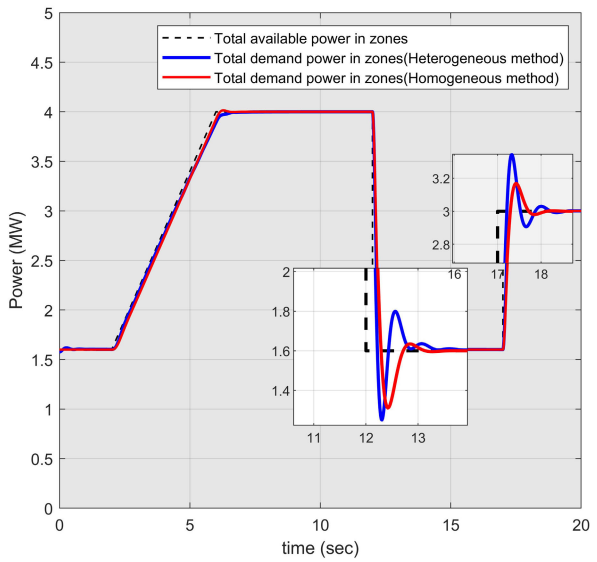

FIGURE 5. Total demand power in zones.

At 12s and 17s when the available power steps down and steps up instantaneously, the load demand calculated by the heterogeneous method produces an overshoot, then remains balanced in one second. The performance of the homogeneous method is better than our method in these two indices, which can be roughly viewed in the small box in Fig.5. However, the overall performance of these two methods are not much different, as shown in Table 2. The statistic in Table 2 represents the percentage of time when the deviation between load demand and available power does not exceed the limit σ.

TABLE 2. Comparison of the overall performance of the two methods.

Method \ σ	$\pm 1\%$	$\pm 2\%$	$\pm 3\%$	$\pm 4\%$	$\pm 5\%$
Homogeneous	72.18%	76%	87.52%	92.78%	94.85%
Heterogeneous	69.11%	83.12%	92.76%	94.06%	94.91%

Next, we will compare the performance of the two methods in zonal level. Fig.6 shows the simulation result of the load demand in each zone, where the red lines are the result of the homogeneous method, and the blue lines are the result of our heterogeneous method, the dash lines indicate the minimum load requirements of each zone.

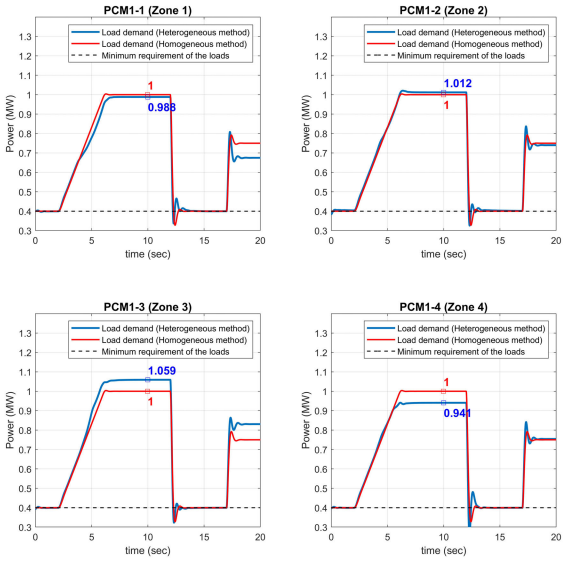

FIGURE 6. Load demand in each zone.

Due to the identical dynamics and the fully-connected communication topology. The load demand of each homogeneous agent is identical as long as their initial state is the same. This could be efficient when the configuration of loads in each zone is identical, and otherwise unbalance between the supply and demand will occur.

As we can see from Table 1, the maximum load ratings from zone 1 to zone 4 is 1MW, 1.07MW, 1.15MW and 0.95MW respectively. At time t=10s when the total available power is 4MW, the load demand of the homogeneous method for each zone is 1MW, zone 4 exceeds its maximum load

requirement and zone 3 does not meet its rated demand. As for the heterogeneous method, the load demand of each zone at t=10s is 0.988MW, 1.012MW, 1.059MW and 0.941MW, which is more consistent with the actual power demand of each zonal load center.

B. LOAD DEMAND OF EACH HETEROGENEOUS AGENT

A more detailed view of the load demand of each heterogeneous agent is shown in Fig.7 and Fig.8. From Table 1 we can figure out the load requirement under three levels of priorities of each PCM.

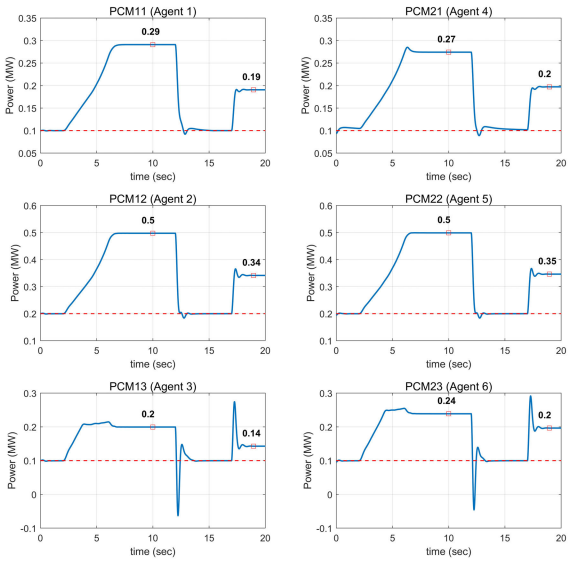

FIGURE 7. Load demand of the agents in zone 1 and zone 2.

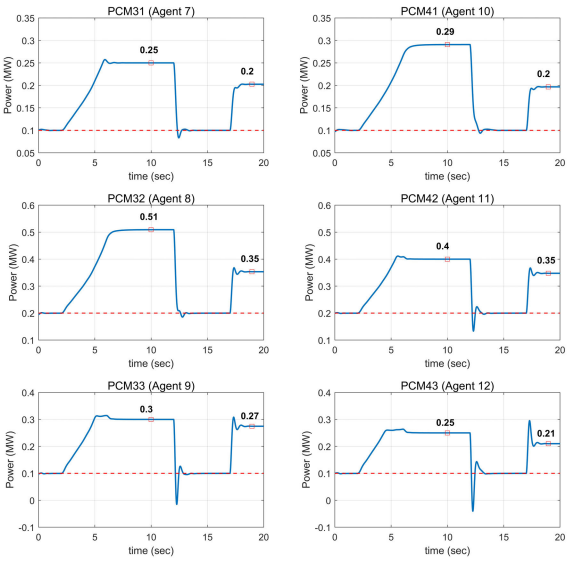

FIGURE 8. Load demand of the agents in zone 3 and zone 4.

For agent 1, agent 2 and agent 3 in zone 1, their maximum load requirements are 0.3MW, 0.5MW and 0.2MW respectively. The calculated load demand for each agent is 0.29MW, 0.5MW and 0.2MW at t=10s, while 0.19MW, 0.34MW and 0.14MW at t=19s. In zone 2, the maximum load requirements for agent 4, agent 5 and agent 6 are 0.28MW, 0.55MW and 0.24MW. At t=10s, the calculated load demand for each agent is 0.27MW, 0.5MW and 0.24MW. And at t=19s, the load demand for them are 0.2MW, 0.35MW and 0.2MW. As for zone 3, the maximum load requirements for agent 7, agent 8 and agent 9 are 0.25MW, 0.6MW and 0.3MW. At t=10s, the calculated load demand for each agent is 0.25MW, 0.51MW and 0.3MW. And at t=19s, the load demand for them are 0.2MW, 0.35MW and 0.27MW. Finally for zone 4, the maximum load requirements for agent 10, agent 11 and agent 12 are 0.3MW, 0.4MW and 0.25MW. At t=10s, the calculated load demand for them are 0.29MW, 0.4MW and 0.25MW. And at t=19s, the load demand for them are 0.2MW, 0.35MW and 0.21MW.

It is obvious from the simulation that, load requirements of the agents are basically met when the available power is relatively sufficient. However, when the available power is insufficient, loads with higher priorities are preferential to be satisfied. Moreover, when load priorities of the agents are the same, agents will reach to consensus with its neighbors according to its respective power requirements and power ramp rates.

C. RETRANSFORMATION OF THE ACTUAL CONTROL VARIABLES

The control variables of the multi-agent system are shown in Fig.9. At t=12s and t=17s, the control variables $u_{ij}(t)$ change intensely since there are step changes in the power available for the zones. Meanwhile, different agents have different lower and upper bound, accordingly, the amount of control applied to the agent is different in order to achieve the collective group objective.

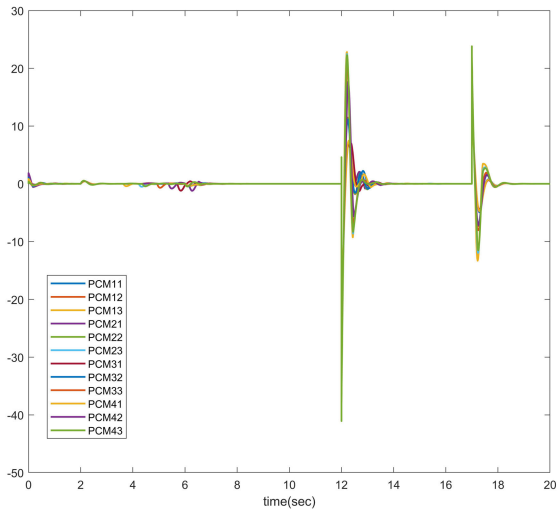

FIGURE 9. Control variable $u_{ij}(t)$ of the multi-agent system.

The real control variables $\hat{u}_{ij}(t)$ of the zonal MVDC SPS can be calculated by (22) once $x_{ij}(t)$, $y_{ij}(t)$ and $u_{ij}(t)$ is

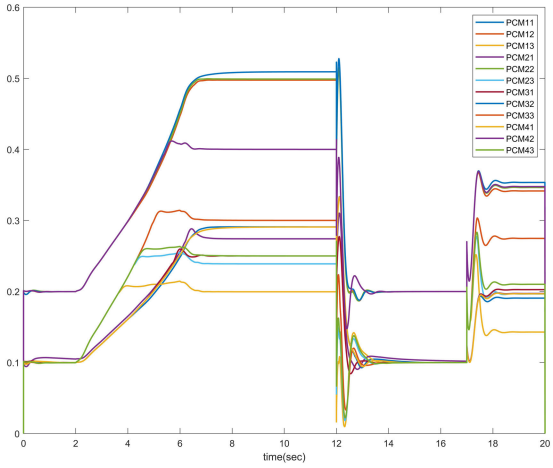

FIGURE 10. Obtained control curve of the actual control variable $\hat{u}_{ij}(t)$.

determined, as shown in Fig.10. Moreover, the priorities of the service loads in zones are categorized into three levels, which are vital, semi-vital and non-vital. Loads with higher priorities are always preferential to be served. Once the load demand of each agent is confirmed, the set of the possible switch status of the service loads can be defined in (24), together with the value of the equivalent loads:

$$\boldsymbol{P_L} = \begin{bmatrix} 0 & 0 & \cdots & 0 \\ 1 & 0 & \cdots & 0 \\ 1 & 1 & \cdots & 0 \\ \vdots & \vdots & \ddots & \vdots \\ 1 & 1 & \cdots & 1 \end{bmatrix}_{(n+1)\times n} \begin{bmatrix} P_{L_1} \\ P_{L_2} \\ \vdots \\ P_{L_n} \end{bmatrix} = \begin{bmatrix} P_L(1) \\ P_L(2) \\ \vdots \\ P_L(n+1) \end{bmatrix} \tag{23}$$

where $[P_{L_1}, P_{L_1}, \cdots, P_{L_1}]^T$ is the rated power of each constant power load, and $[P_L(1), P_L(2), \cdots, P_L(n+1)]^T$ is the load values for all the possible switch status sequence.

The control signal $\hat{u}(t)$ can be calculated through (23) when $x(t)$, $y(t)$ and $u(t)$ are confirmed. Then the switch status can be determined by comparing $\hat{u}(t)$ with the equivalent load value interval:

$$P_L(m) \leq \hat{u}(t) \leq P_L(m+1) \tag{24}$$

Then switch status σ can be determined, for $i = 1 : m, \sigma_i = 1$, otherwise $\sigma_i = 0$.

VI. DISCUSSION

Compared with the homogeneous method, our improvements are mainly reflected in both modelling and algorithms.

First of all, DC-DC converters with different voltage levels are modelled as heterogeneous agents, rather than the entire power conversion module of zonal load center as a homogeneous agent. As a result, the load at different voltage level can be controlled individually according to their load ratings and priorities, and the modelling is more precise.

Secondly, a modified navigational feedback, with the function of confining the lower and upper bound of the load demand of each agent, is adopted in the flocking based cooperative control protocol for the heterogeneous multi-agent system. For the three terms in the control protocol, the artificial potential function drives the agents towards a collective objective, which is to maximize load demand in accordance with the available power and system operating constraints. The Laplacian matrix acts as a consensus term to simulate the in-zone information exchange of the agent with its neighbors, and to ensure the well distribution of the load demand. Then, the modified navigational feedback term acts as a virtual leader to ensure each agent's changing rate is consistent with the available power, and the load demand of each agent should be within certain bound.

The numerical simulation demonstrates that, our method has superior performance in converter level especially when the configuration of load ratings is different, and the calculated load demand is closer to the actual power demand.

VII. CONCLUSION

In this paper, a heterogeneous multi-agent based load demand management method for zonal MVDC SPS was presented. The similarity of zonal load centers' architecture and the differences between DC converters at various voltage levels were considered in the modelling of the agents, and the zonal MVDC SPS was abstracted into a heterogeneous multi-agent system.

A flocking based cooperative control protocol was developed for the heterogeneous multi-agent system to achieve the group objective, which is maximizing load demand in zones while satisfying system operating constraints and load priorities. Besides, a modified feedback was adopted in the control protocol to guarantee that each agent operates within feasible range.

The simulation results indicated that the load demand and the power generation can be matched accurately in affordable time subjecting to the available power capacity constraints and the MVDC bus constraints. The priorities of the loads can also be considered so that the loads with higher priorities are ensured to be served first. It is worth noting that the numerical simulations represented typical operating conditions, including the continuous change in ship speed and the adoption of pulse loads in MVDC SPS.

Our future research will investigate the operating risk during the structural changes of the power system, and explore the applications of the proposed method, as at present the multi-agent method is considered to be applied in a hardware-in-the-loop simulation environment.

REFERENCES

[1] N. Doerry, "Naval power systems: Integrated power systems for the continuity of the electrical power supply," *IEEE Electrific. Mag.*, vol. 3, no. 2, pp. 12–21, Jun. 2015.
[2] T. V. Vu, D. Gonsoulin, F. Diaz, C. S. Edrington, and T. El-Mezyani, "Predictive control for energy management in ship power systems under high-power ramp rate loads," *IEEE Trans. Energy Convers*, vol. 32, no. 2, pp. 788–797, Jun. 2017.
[3] N. Doerry and J. Amy, "Dc voltage interface standards for naval applications," in *Proc. IEEE Electr. Ship Technol. Symp. (ESTS)*, Jun. 2015, pp. 318–325.

[4] R. Soman, M. M. Steurer, T. A. Toshon, M. O. Faruque, and R. M. Cuzner, "Size and weight computation of MVDC power equipment in architectures developed using the smart ship systems design environment," *IEEE J. Emerg. Sel. Topics Power Electron.*, vol. 5, no. 1, pp. 40–50, Mar. 2017.

[5] N. Doerry, "Zonal ship design," *Naval Eng. J.*, vol. 118, no. 1, pp. 39–53, Jan. 2006.

[6] *IEEE Recommended Practice for 1 kV to 35 kV Medium-Voltage DC Power Systems on Ships*, Standard 1709-2010, 2010, pp. 1–54.

[7] *IEEE standard for power electronics open system interfaces in zonal electrical distribution systems rated above 100 kw*, Standard 1826-2012, 2012, pp. 1–46.

[8] K. H. Ng and G. B. Sheble, "Direct load control-a profit-based load management using linear programming," *IEEE Trans. Power Syst.*, vol. 13, no. 2, pp. 688–694, May 1998.

[9] J. M. Lujano-Rojas, C. Monteiro, R. Dufo-López, and J. L. Bernal-Agustín, "Optimum residential load management strategy for real time pricing (RTP) demand response programs," *Energy Policy*, vol. 45, pp. 671–679, Jun. 2012.

[10] D. L. Ha, F. F. De Lamotte, and Q. H. Huynh, "Real-time dynamic multilevel optimization for demand-side load management," in *Proc. IEEE Int. Conf. Ind. Eng. Eng. Manage.*, Dec. 2010, pp. 945–949.

[11] X. Feng, K. L. Butler-Purry, and T. Zourntos, "Multi-agent system-based real-time load management for all-electric ship power systems in DC zone level," *IEEE Trans. Power Syst.*, vol. 27, no. 4, pp. 1719–1728, Nov. 2012.

[12] K. Huang, D. A. Cartes, and S. K. Srivastava, "A multiagent-based algorithm for ring-structured shipboard power system reconfiguration," *IEEE Trans. Syst., Man, Cybern. C, Appl. Rev.*, vol. 37, no. 5, pp. 1016–1021, Sep. 2007.

[13] Y. Xu and W. Liu, "Novel multiagent based load restoration algorithm for microgrids," *IEEE Trans. Smart Grid*, vol. 2, no. 1, pp. 152–161, Mar. 2011.

[14] S. D. J. Mcarthur, E. M. Davidson, V. M. Catterson, A. L. Dimeas, N. D. Hatziargyriou, F. Ponci, and T. Funabashi, "Multi-agent systems for power engineering applications—Part I: Concepts, approaches, and technical challenges," *IEEE Trans. Power Syst.*, vol. 22, no. 4, pp. 1743–1752, Nov. 2007.

[15] J. M. Solanki and N. N. Schulz, "Using intelligent multi-agent systems for shipboard power systems reconfiguration," in *Proc. 13th Int. Conf., Intell. Syst. Appl. Power Syst.*, Nov. 2005, p. 3.

[16] L. Liu, K. P. Logan, D. A. Cartes, and S. K. Srivastava, "Fault Detection, Diagnostics, and Prognostics: Software Agent Solutions," *IEEE Trans. Veh. Technol.*, vol. 56, no. 4, pp. 1613–1622, Jul. 2007.

[17] X. Feng, K. L. Butler-Purry, and T. Zourntos, "Real-time electric load management for dc zonal all-electric ship power systems," *Electric Power Syst. Res.*, vol. 154, pp. 503–514, 2018.

[18] W. Du, G. Yang, J. Bai, C. Pan, and Q. Gong, "Reliability evaluation of a zonal shipboard power system based on minimal cut set," in *Proc. Int. Conf. Swarm Intell.* Cham, Switzerland: Springer, 2016, pp. 563–572.

[19] M. Babaei, J. Shi, and S. Abdelwahed, "A survey on fault detection, isolation, and reconfiguration methods in electric ship power systems," *IEEE Access*, vol. 6, pp. 9430–9441, 2018.

[20] F. M. Uriarte and C. Dufour, "Multicore methods to accelerate ship power system simulations," in *Proc. IEEE Electr. Ship Technol. Symp. (ESTS)*, Apr. 2013, pp. 139–146.

[21] M. S. Agamy, D. Dong, L. J. Garcès, Y. Zhang, M. E. Dame, X. Wu, and Y. Pan, "A high power medium voltage resonant dual active bridge for MVDC ship power networks," *IEEE J. Emerg. Sel. Topics Power Electron.*, vol. 5, no. 1, pp. 88–99, Jan. 2017.

[22] P. Kundur, J. Paserba, V. Ajjarapu, G. Andersson, A. Bose, C. Canizares, N. Hatziargyriou, D. Hill, A. Stankovic, C. Taylor, T. Van Cutsem, and V. Vittal, "Definition and classification of power system stability IEEE/CIGRE joint task force on stability terms and definitions," *IEEE Trans. Power Syst.*, vol. 19, no. 3, pp. 1387–1401, Aug. 2004.

[23] R. W. Erickson and D. Maksimović, *Fundamentals of Power Electronics*. Springer, 2007.

[24] A. Kwasinski and C. N. Onwuchekwa, "Dynamic behavior and stabilization of dc microgrids with instantaneous constant-power loads," *IEEE Trans. Power Electron.*, vol. 26, no. 3, pp. 822–834, Mar. 2011.

[25] A. Davoudi, J. Jatskevich, and T. De Rybel, "Numerical state-space average-value modeling of PWM DC-DC converters operating in DCM and CCM," *IEEE Trans. Power Electron.*, vol. 21, no. 4, pp. 1003–1012, Jul. 2006.

[26] R. Olfati-Saber, "Flocking for multi-agent dynamic systems: Algorithms and theory," *IEEE Trans. Autom. Control*, vol. 51, no. 3, pp. 401–420, Mar. 2006.

[27] R. Olfati-Saber, J. A. Fax, and R. M. Murray, "Consensus and cooperation in networked multi-agent systems," *Proc. IEEE*, vol. 95, no. 1, pp. 215–233, Jan. 2007.

WENZENG DU received the bachelor's degree from the Department of Automation, Shanghai Jiao Tong University, in 2014, where he is currently pursuing the Ph.D. degree. He is currently a member of the Collaborative Innovation Center for Advanced Ship and Deep-Sea Exploration, Shanghai, China. His current research interests include load management, power flow calculation, stability analysis, and the control of shipboard power systems.

GENKE YANG was born in Shanxi, China. He received the B.S. degree in mathematics from Shanxi University, in 1984, the M.S. degree in mathematics from Xi'nan Normal University, in 1987, and the Ph.D. degree in systems engineering from Xi'an Jiaotong University, in 1998.

He has been a full-time Professor with the Department of Automation, Shanghai Jiao Tong University, Shanghai, China. He is currently a member of the Collaborative Innovation Center for Advanced Ship and Deep-Sea Exploration, Shanghai. His research interests include supply chain management, logistics, production planning and scheduling, discrete event dynamics systems, and computer integrated manufacturing.

CHANGCHUN PAN received the M.S. degree in control science and engineering from the Nanjing University of Aeronautics and Astronautics, in 2004, and the Ph.D. degree in system engineering from Shanghai Jiao Tong University, in 2009.

From 2010 to 2011, he was a Postdoctoral Researcher with the Department of Chemical Engineering, National Tsinghua University, Hsinchu, Taiwan. In October to December 2015, he was a Visiting Scholar with the Massachusetts Institute of Technology, Cambridge, MA, USA. He has been an Associate Professor with the Department of Electronic Engineering, Shanghai Jiao Tong University. His current research interest includes production scheduling and optimization, industrial process control, and location-based data analysis.

PEIFENG XI received the B.S. degree in electronic engineering from Shanghai University, in 2004, and the M.S. degree in electronic engineering from Shanghai Jiao Tong University, in 2010.

He is currently with the Shanghai Electrical Apparatus Research Institute. He is also a member of the Shanghai Key Laboratory of Smart Grid Demand Response, Shanghai, China. His current research interests include smart grid, demand response, and energy management.